Pergamon

Tetrahedron 58 (2002) 10151–10158

TETRAHEDRON

Conformational profile, energy barriers and optical properties of quinquethiophene-*S*,*S*-dioxides

Alessandro Bongini,[a,*] Giovanna Barbarella,[b] Laura Favaretto,[b] Giovanna Sotgiu,[b] Massimo Zambianchi[b] and Daniele Casarini[c]

[a]*Dipartimento Chimico G. Ciamician, Università di Bologna,Via Selmi 2, 40126 Bologna, Italy*
[b]*CNR-ISOF, Via Gobetti 101, 40129 Bologna, Italy*
[c]*Dipartimento Chimico, Università della Basilicata, Via N. Sauro 85, 85100 Potenza, Italy*

Received 19 July 2002; revised 4 October 2002; accepted 24 October 2002

Abstract—Theoretical calculations, dynamic NMR experiments and absorption and photoluminescence data in solution are reported for a series of quinquethiophene *S*,*S*-dioxides substituted with alkyl groups of variable size and steric hindrance. Ab initio B3LYP/6-31G* and force field MM3 theoretical calculations show that the energy barriers for rotation around the inter-ring C–C bonds amount to a few kcal/mol even in the presence of very bulky substituents such as the cyclohexyl group. Dynamic NMR data were in agreement with the results of theoretical calculations. It was found that changing the steric hindrance of the substituents leaves the emission and photoluminesce properties unaltered. However, the photoluminesce intensities and wavelengths of all compounds were found to be very sensitive to solvent variations.

Thiophene oligomers are among the most studied conjugated materials both as models for the corresponding polymers and as materials interesting in themselves for application in a variety of organic devices.[1–6]

Selective oxidation of one or more of the thienyl sulfurs of conventional thiophene oligomers deeply affects their electronic properties, in particular their electron affinity[7] and their photoluminescence quantum yield in the solid state.[8a] Recently, widely tunable electroluminescence emission and good electroluminescence efficiency have been demonstrated for these types of compounds, owing to the increased photoluminesce efficiency and electron affinity.[8b–d]

It has been found that while in the solid state the photoluminescence quantum yields of oligothiophene-*S*,*S*-dioxides may attain values up to 70%,[8a] in solution their photoluminescence quantum yields drop by one or two orders of magnitude.[8d] This indicates that the non-radiative mechanisms for energy relaxation from the excited state of oligothiophene-*S*,*S*-dioxides are different from those of the corresponding conventional oligothiophenes (which display high photoluminescence efficiencies in solution but not in the solid state) and suggests that conformational mobility might play an important role in determining the photoluminescence behavior.

However, while many accurate studies on conventional thiophene oligomers have been reported,[9] very little is known so far about the conformational properties of oligothiophene-*S*,*S*-dioxides. Since a deeper understanding of the relationships between photoluminescence properties and molecular structure is crucial to the design and synthesis of new, higher performance materials, we report in this paper a theoretical and experimental study of the conformational properties of a homogeneous series of these compounds. In particular, we have explored the effect exerted by the introduction of bulky substituents into the molecular backbone on the inter-ring energy barriers and conformational mobility.

To this purpose, compounds **1**–**4**—whose molecular structure is reported in Scheme 1—were taken into account. Their conformational profile was estimated by the aid of B3LYP/6-31G* ab initio and MM3 theoretical calculations

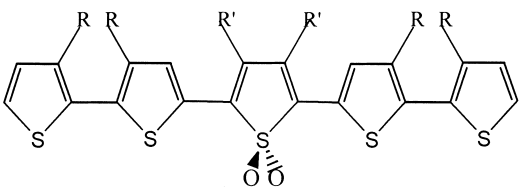

Scheme 1. Oligothiophene-*S*,*S*-dioxides **1**–**4**. R=R′=methyl (**1**); R=methyl, R′=*n*-hexyl (**2**); R=cyclohexyl, R′=*n*-hexyl (**3**); R=R′=neopentyl (**4**).

Keywords: conformation; thiophenes; theoretical studies; optical properties.

* Corresponding author. Tel.: +39-051-2099589; fax: +39-051-2099456; e-mail: bongini@ciam.unibo.it

0040–4020/02/$ - see front matter
PII: S0040-4020(02)01398-4

on shorter sub-systems and the energy barriers to conformational interconversion compared to those obtained from low temperature proton NMR experiments.

Finally, absorption and photoluminescence data in two solvents of different viscosity (methylene chloride and decalin) are reported for **1**–**4** and the optical properties of these compounds discussed in the light of their conformational characteristics.

1. Results

1.1. Theoretical calculations

1.1.1. Ab initio torsional profiles and MM3 geometries and energies of model dimers and trimers. We have recently demonstrated by B3LYP/6-31G* ab initio calculations that, for a correct description of the torsional potential profiles of thiophene oligomers, correlation energy contributions have to be taken into account.[9a] However, the size of compounds **1**–**4** prevents the possibility to perform ab initio calculations on the entire molecule at such a level and some approximations are required.

Looking at the molecular structure of **1**–**4** (Scheme 1) it is seen that there are two different types of junctions between the aromatic rings, namely the one linking the terminal thiophene moieties and the one linking the oxygenated moiety to the adjacent thiophene rings. Such junctions can be modeled by the dimers 3,3′-dimethyl-2,2′-bithiophene ($TTMe_2$) and 3-methyl-2,2′-bithiophene-1,1-dioxide (TOMe), respectively (Scheme 2).

The inter-ring torsional profile of $TTMe_2$ has already been calculated by us at the B3LYP/6-31G* level.[9a] We have thus calculated the inter-ring torsional profile of TOMe at the same calculation level and the results are illustrated in Fig. 1 together with those of $TTMe_2$ for comparison. The inter-ring torsional angle is varying from 0° for fully planar *syn* conformation to 180° for fully planar *anti* conformation. The critical points were checked by a frequency analysis. The minimum points showed no imaginary frequency. The maximum points showed one imaginary frequency, which resulted consistent with the inter-ring torsional path.

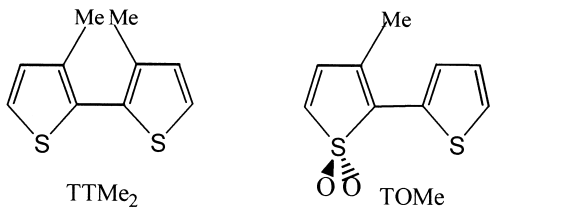

Scheme 2. Dimers used in ab initio calculations.

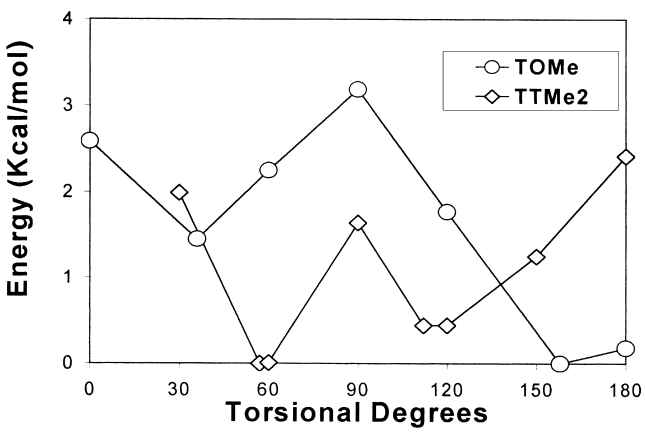

Figure 1. Ab initio torsional profile of TOMe and $TTMe_2$ (Scheme 2).

Fig. 1 shows that, for TOMe, there is a principal minimum for ω=158° corresponding to an *anti* orientation between the two rings and a less populated minimum for ω=36° corresponding to a *syn* orientation.

The region between the two *anti* forms (ω=+158° and −158°) is very flat indicating a very low energy barrier to interconversion between the two forms. The energy barriers for the interconversion between the two *syn* forms (ω=+36° and −36°) and between the *syn* and *anti* forms are larger but still small (1.14 and 3.19 kcal/mol, respectively).

The comparison of the energy profile of TOMe with that of $TTMe_2$, which is described by two almost equally populated *syn* and *anti* conformations, shows that the latter is characterized by a markedly more twisted geometry than the former and by a different profile of the energy barriers (for $TTMe_2$ the largest energy barrier is that between the two *anti* forms. The direct rotation from +*syn* to −*syn* through a planar *cis* conformation would necessitate the two methyl groups passing one into the other and is not a valid torsional path). However, both $TTMe_2$ and TOMe do not display energy barriers higher than 5 kcal/mol.

In order to estimate the trend of variation in energies and geometries as the size of the alkyl groups R and R′ increases progressively, MM3 mechanical calculations—which are known to give reliable geometry and energy values—were carried out for fragments TTR_2 and $TOTR'_2$ (Scheme 3). Since the standard MM3 package does not contain the parametrization constants for the torsional angles between the thienyl and sulfonyl rings we had to derive such constants first. The parametrization was carried out in such a way as to have the best fitting with the ab initio results shown in Fig. 1. We found that by assigning to the torsional constants V1, V2 and V3 the values 0,0,5 −7,4,5 and 0,99,0 for the atom types 18-2-2-42 (Sox–C–C–S), 42-2-2-42 (S–C–C–S) and 1-2-2-2 (Csp^3–Csp^2–Csp^2–Csp^2), respectively, a satisfactory reproduction of ab initio structures was obtained. Indeed, the torsional inter-ring angles and the relative energies of the two minima of TOMe

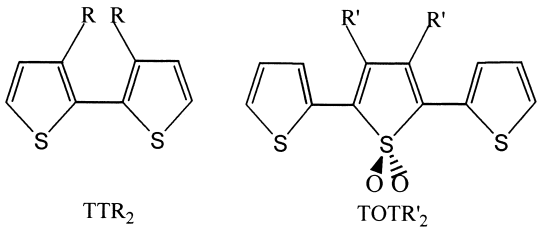

Scheme 3. Dimers and trimers used for MM3 calculations. R=methyl, cyclohexyl, neopentyl; R′=methyl, *n*-hexyl, neopentyl.

Table 1. MM3 energies (E, kcal/mol) of $TOTR'_2$ as a function of the inter-ring angle (ω, °)

R′ methyl	ω,ω'	0,0 fixed	±(38,38)	±(38,150)	±(150,150)	180,180 fixed
	E	79.9	75.2	74.3	73.3	74.3
R′ *n*-hexyl	ω,ω'	0,0 fixed	±(47,47)	±(47,154)	±(154,154)	180,180 fixed
	E	86.7	82.4	81.3	80.5	81.0
R′ neopentyl	ω,ω'	0,0 fixed	−48,−48	−48,+134	+134,+134	180,180 fixed
	E	95.0	83.8	83.2	82.6	91.1

Table 2. MM3 energies (E, kcal/mol) of TTR_2 as a function of the inter-ring angle (ω, °)

R methyl	ω	±48	±111	180 fixed
	E	42.0	41.5	49.3
R cyclohexyl-(eqeq)	ω	±61	±110	180 fixed
	E	52.1	51.3	66.1
R neopentyl (A)	ω	+70	−132	180 fixed
	E	48.5	52.5	61.0
R neopentyl (B)	ω		±108	180 fixed
	E		48.8	61.1

and $TTMe_2$ calculated by MM3 are very similar to those calculated ab initio (TOMe conformations: *syn* ω=32°; *trans* ω=164°, ΔE=1.4 kcal/mol). Moreover, the relative trends of the energy barriers for the planar conformations of TOMe and $TTMe_2$ are reproduced. As a further control, an ab initio calculation on the *syn*,*syn* and *anti*,*anti* conformations of $TOTMe_2$ was performed at B3LYP/6-31G* level and the results (*syn*,*syn* ω=+41,−41; *anti*,*anti* ω=+153,−153; ΔE=2.3 kcal/mol) are in good agreement with those obtained by MM3 calculation (Table 1). MM3 failed in the reproduction of the *syn*–*anti* interconversion energy barriers. The MM3 calculated profile between the *syn* and the *anti* conformers is very flat, and on imposing fixed inter-ring angles ω=90° the values of the energy barrier are too low to be meaningful and then are not reported.

The results of MM3 calculations on $TOTR'_2$ and TTR_2 are reported in Tables 1 and 2, in which the minimum energy conformations are shown, together with the planar conformations obtained by imposing to the inter-ring angles the fixed values of 0° or 180°, respectively. Table 1 shows that in trimers $TOTR'_2$, the *anti*,*anti* conformers are always the most stable ones. The energy barrier between the +*syn* and −*syn* forms (or between the +*anti* and −*anti* forms) was obtained dividing by two the difference between the energy of the *syn*,*syn* (or *anti*,*anti*) conformation and the energy of the planar 0,0 (or 180,180) conformation.

For R′=methyl and R′=*n*-hexyl, the energy barrier between the two *anti*–*anti* forms is very low, not exceeding 0.5 kcal/mol, whereas the energy barrier between the two *syn*–*syn* forms amounts to more than 2 kcal/mol. Due to the larger size of the substituents, for the trimer with R′= neopentyl, both energy barriers are markedly higher, amounting to 5–6 kcal/mol. This behavior can be explained by taking into account that the neopentyl group has a preferred conformation in which the *t*-butyl moieties of the neopentyl substituents are placed perpendicularly up and down the plane of the sulfonyl ring, as depicted in Scheme 4. The rotation of the terminal ring generates two different energy minima +*anti* and −*syn* corresponding to the forms characterized by the C–H bonds (−*syn*) or S atoms (+*anti*) of the thiophene ring being on the other side to the face where the *t*-butyl group is located.

The +*anti* to −*syn* profile is of course equi-energetic with the enantiomeric −*anti* to +*syn* profile in which the *t*-butyl residues are on the other side of the sulfonyl ring. As the two *t*-butyl residues cannot stay on the same side for steric reasons, a synchronous rotation of the two neopentyl groups must occur to pass from one profile to the other.

Table 2 shows that also in dimers TTR_2 the *anti* orientation is always energetically favored over the *syn* one.

Due to greater steric interactions between the substituents, the inter-ring junction is more twisted and the energy barrier between the two *anti* forms is higher than in the trimers. Concerning the cyclohexyl substituents, which can be either linked equatorially or axially to the thiophene rings, Table 2 only reports the energies relative to the diequatorial dimer, as axial substitutions merely increases the energy of all maxima and minima by 4 kcal/mol (8 kcal/mol for axial disubstitution).

The dimer bearing two neopentyl substituents displays two different torsional profiles depending on whether the *t*-butyl moieties, which are placed perpendicularly to the plane of the thienyl rings, are on the same side (case A) or on opposite sides (case B), as shown in Scheme 4. In this case, the two neopentyl groups do not interfere with each other,

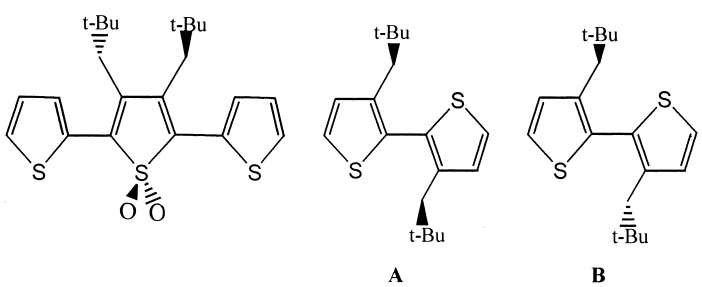

A B

Scheme 4. Relative orientations of the *t*-butyl moieties of the neopentyl substituents.

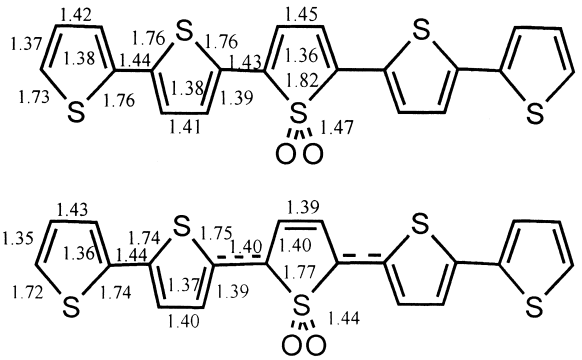

Scheme 5. Ab initio optimized geometries of the preferred conformation for the ground and excited states of unsubstituted quinquethiophene-*S*,*S*-dioxide.

and it is possible to pass from the A to the B profile simply by rotation of one single neopentyl group.

1.1.2. ZINDO/S calculations of absorption and emission wavelengths of unsubstituted quinquethiophene-*S*,*S*-dioxide. To have an insight into the optical properties of compounds **1**–**4** a ZINDO/S analysis was performed on the ab initio optimized geometry of the all-*anti* preferred conformation[8f] of unsubstituted quinquethiophene-*S*,*S*-dioxide (see Scheme 1, R=R′=H) taken as model compound.

The ab initio calculations were performed at the 6-31G* level, using a hybrid density functional B3LYP for the ground state and a CI-Singles correlation method for the first excited state.

The ground state was found to have an almost planar geometry, with an inter-ring torsional angle ω=168° and an inter-ring distance of 1.428 and 1.445 Å for the thienyl dioxide–thienyl and thienyl–thienyl moieties, respectively.

The excited state was found to have a full planar geometry with a quinoid structure mainly localized on the three central rings as shown, inter alia, by the marked decrease of the inter-ring distance between the thienyl dioxide and the thienyl rings, which changes from 1.428 Å in the ground state to 1.403 Å in the excited state whilst the thienyl–thienyl distance is unchanged (Scheme 5).

Moreover, the excited state is characterized by a greater polar character as shown by the change in dipole moments, which vary from 3.78 D in the ground state to 4.65 D in the excited state.

The ZINDO/S calculated maximum absorption wavelength, λ_{max}=507 nm, originates from a HOMO–LUMO π–π^* transition with the coefficients of the orbitals mainly localized on the skeleton carbon atoms. In consequence, the absorption band is very sensitive to torsional distortions of the ring chain. The λ_{max} value wavelength falls to 440 nm when the calculations are performed on imposing to the ab initio calculated ground geometry the MM3 calculated inter-ring torsion angles typical of the substituted

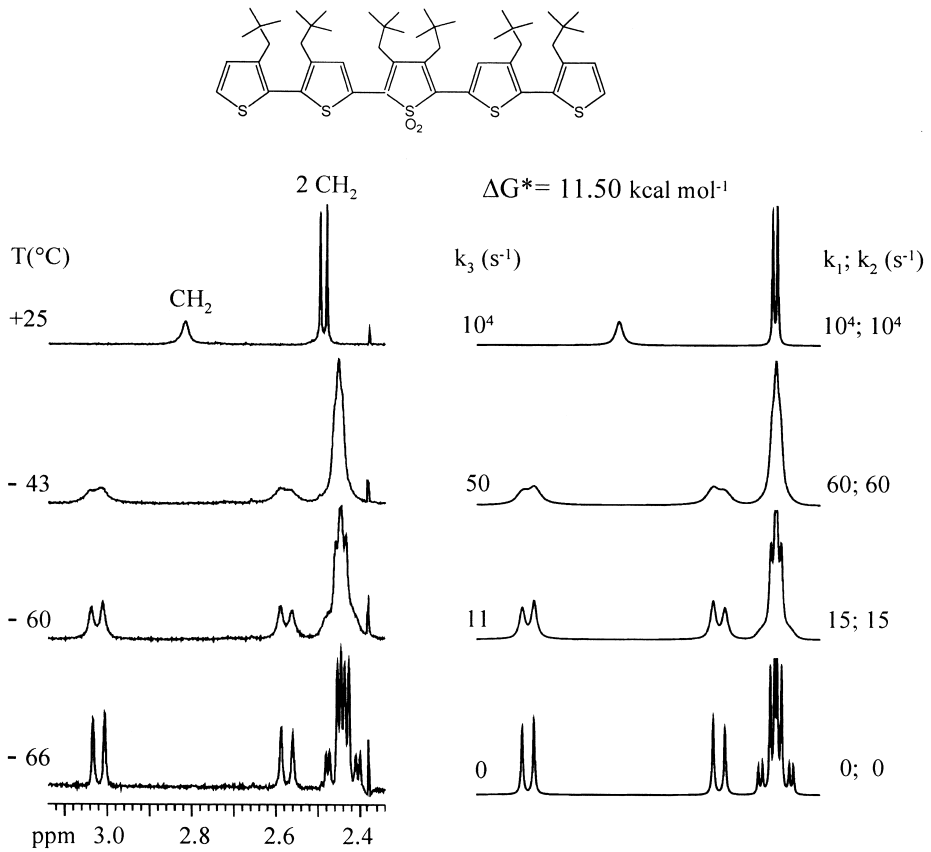

Figure 2. Left: experimental ^{1}H NMR spectra at 400 MHz of the aliphatic region of **4** in CD_2Cl_2 at different temperatures. Right: simulated spectra.

compounds (ω=150° and 110° for the thienyl dioxide–thienyl and thienyl–thienyl junctions, respectively).

The ZINDO/S calculated wavelength emission is λ_{PL}= 574 nm and the emission band has the same $\pi-\pi^*$ character as that of the absorption band.

1.2. Dynamic NMR

Samples in $CHF_2Cl-CF_2Cl_2$ (1:1) were prepared for compounds **1**–**3** and ^{1}H VT experiments carried out, but in all cases the signals pertaining to the thienyl hydrogens remained substantially unchanged even at −140°C except that for **1**, which precipitated below T=−80°C.

Compound **4** was dissolved in CD_2Cl_2 ($\approx10^{-4}$ M) and slowly cooled in several steps down to −95°C. The changes observed in the proton spectra are shown in Fig. 2.

At +25°C, the proton spectrum of **4** showed only half signals for the ring hydrogens and the neopentyl groups in the molecule, thus indicating the presence of symmetry element that, bisecting the central ring, divides the molecule in two equivalent halves.

The two sharp signals at 2.38 and 2.40 ppm were assigned to the methylenes of the neopentyl groups bonded to the outer thienyl rings by comparison with the observed shifts of the neopentyl methylenes in the 3,3′-dineopentyl-2,2′-bithiophene.[8a] The remaining broad signal at 2.80 ppm was assigned to the methylene of the neopentyl bonded to the central ring.

On lowering the temperature, the broad methylene signal at 2.8 ppm decoalesces at −15°C and splits into a sharp AB quartet (J=14.0 Hz) below −60°C. In addition, the other two methylene signals broaden, at −40°C, and split, below −60°C, into two sharp and overlapped AB quartets (J= 13.8 Hz).

This indicates that the neopentyl groups are tilted from coplanarity with the averaged molecular plane of the thiophene rings and that the barriers to rotation about the bonds methylene–thienyl are quite high. Indeed, by simulating the changes of the CH_2 line shapes with the temperature the kinetic constants were achieved and then an energy barrier of 11.50±0.15 kcal/mol involved in the observed rotational process of the neopentyl groups was obtained.

In order to slow down other rotational processes ^{1}H spectra of **4** in $CHF_2Cl-CF_2Cl_2$ (1:1) were taken at much lower temperatures. At −145°C, the minimum temperature reached owing to solubility problems, the aromatic and the *t*-butyl signals remained substantially unchanged suggesting that such rotational barriers are lower than 5 kcal/mol.

1.3. Optical properties

Table 3 shows the absorption and photoluminescence wavelengths of compounds **1**–**4** in two different solvents, methylene chloride (MC) and decalin (D), together with the molar absorption coefficients (ε) and the photoluminescence (PL) intensities measured for 10^{-5} M solutions. The two solvents were chosen because of their very different polarities and viscosities (dielectric constant 8.9 and 2.2; dipole moment 1.6 and 0 D; viscosity 0.4 and 2–3 cp, respectively).

Table 3. Maximum absorption (λ_{max}, nm) and emission(λ_{PL}, nm) wavelengths, molar extinction coefficients (ε, $cm^{-1}\,M^{-1}$) and relative photoluminescence intensities (I) of compounds **1**–**4** in methylene chloride (MC) and decalin (D)

	Solvent	λ_{max}	ε	λ_{PL}	I
1	MC	445	22387	591	1
	D	444	25704	570	20
2	MC	453	23988	590	2
	D	451	22387	569	32
3	MC	452	24547	581	4
	D	450	26915	554	35
4	MC	444	19498	580	3
	D	439	19953	557	22

The most remarkable feature shown in Table 3 is that there is one order of magnitude increase in the photoluminescence intensities of **1**–**4** on going from methylene chloride to decalin while the wavelengths, λ_{PL}, decrease by 20–30 nm, contrary to λ_{max} which is unaffected by the change of solvent. Since the concentrations of **1**–**4** are the same in both solvents and the molar absorption coefficients are also very similar, it is likely that the increase in photoluminescence intensities is mainly due to the increase in photoluminescence quantum yields.

2. Discussion

Theoretical calculations show that quinquethiophene-*S*,*S*-dioxides are characterized by very high conformational mobilities. These kinds of compounds are more planar than the corresponding conventional oligothiophenes but the energy barriers for conversion from one form to the other are very low and they exist in solution as families of rapidly interconverting conformers of nearly the same energies.

According to theoretical calculations, the energy barriers for ring rotation around the C–C bonds linking the thienyl dioxide moiety and the adjacent thienyl rings are very low. The energy barriers for ring rotation around the C–C bond linking the terminal thienyl rings are higher, but these values are still low enough to allow the molecules to be conformationally mobile at room temperature despite the presence of bulky substituents.

Low temperature dynamic proton NMR experiments confirmed the results of theoretical calculations. Indeed, even at temperatures as low as −140°C no freezing of the conformational equilibria was observed. The only rotations frozen at low temperature were the rotations of the methylene groups of the neopentyl substituents, shown in Fig. 2 and easily interpreted with the aid of MM3 calculations. The spectra of Fig. 2 show that the four neopentyl substituents of compound **4** experience similar steric environments and MM3 calculations allow it to be established that the origin of the energy barriers measured

by proton NMR is due both to steric interactions occurring between the bulky neopentyl groups and the thienyl rings and to steric interactions occurring between the neopentyl substituents themselves. Although these steric interactions also contribute to the distortions of the rings from coplanarity, conferring on the molecule a helix-like shape, they do not prevent the molecule from interchanging between the different forms of the whole family of *syn*–*anti* arrangements of adjacent rings.

Table 3 shows that the different size of the substituents does not substantially affect the spectroscopic properties of **1**–**4** compounds.

The high values of the molar extinction coefficients of the absorption bands indicate the $\pi-\pi^*$ nature of the transition that ZINDO/S calculations show to be HOMO–LUMO in character, as found in trimers analogues.[8g,10] The wavelengths of the maximum absorption of π bands is very sensitive to distortions from planarity of the conjugated system. The invariance of λ_{max} in **1**–**4** shows that the inter-ring twisting induced in these compounds by the substituents is almost the same.

In compounds **1**–**4**, the similarity of λ_{PL} in the same solvent shows that also in the excited state the different size of the substituents does not affect the inter-ring energy barriers and the geometry of the molecular backbones. The strong red shift (5600 cm^{-1}) found between absorption and emission bands indicates a more planar structure in the excited state, in agreement with ab initio calculations which predict a planar quinoid geometry for the excited state of the model unsubstituted pentamer (Scheme 5). Moreover, the strict concordance observed between the ZINDO/S λ_{PL} value calculated on the ab initio geometry (574 nm) and the experimental values found for **1**–**4** in decalin (550–570 nm) further supports the planar structure of the excited state.

The red shift of about 600 cm^{-1} of λ_{PL} found on going from decalin to methylene chloride for all compounds indicates the occurrence of some interaction between the solute and the solvent in the excited state. Ab initio calculations show that the excited state is more polar than the ground state. Upon excitation, the smaller and more polar molecules of dichloromethane have time to rearrange around the excited molecule, some energy is dissipated and λ_{PL} increases.[11]

The most important variation observed for all compounds on passing from methylene chloride to decalin is the marked increase in PL intensities, independent of the size of the substituents. It is known that the dominant non-radiative relaxation pathway for oligothiophene-*S*,*S*-dioxides is internal conversion (IC) rather than inter system crossing (ISC).[8e,10] The IC mechanism is strongly dependent on the coupling with vibro-rotational quanta of the excited state. In these molecules, the inter-ring torsional twisting mode is the coupling type that is to be considered. The low photoluminescence intensities measured in dichloromethane for **1**–**4** show that in these compounds the IC mechanism is very efficient. It is known that, when PL depends on IC, PL quantum yields of flexible molecules increase in viscous media as decalin. In a previous work we could infer that in oligothiophene-*S*,*S*-dioxides the first excited state is mainly localized on the oxygenated moiety.[8e] Ab initio calculations confirm this finding also for **1**–**4** compounds, but, even if the quinoid form assumed in the excited state is more rigid than the aromatic structure of the ground state, these compounds are still sufficiently conformationally mobile around the central oxygenated part to have an efficient non-radiative relaxation. Only the increase in the viscosity of the medium has the effect of slowing down the conformational mobility and therein strongly increases the PL efficiency. Energy barriers induced by the substituents are not sufficiently high to hinder the conformational mobility. Only strongly hindering groups as *t*-butyl can freeze the conformational mobility, but they are known to prevent the planarity, and hence the conjugation, in the molecule and cut off all luminescent effects.[8a]

3. Conclusions

Theoretical and experimental data show that the conformational mobility of substituted quinquethiophene-*S*,*S*-dioxides is not blocked even by the use of bulky substituents such as cyclohexyl or neopentyl groups. As oligothiophene-*S*,*S*-dioxides are known to be relaxed from the excited state by IC pathways, the conformational mobility of **1**–**4** compounds makes this mechanism very efficient and strongly decreases the photoluminescence of these compounds in solution. The size of the alkyl substituents is therefore not very important for the photoluminescence efficiency of these compounds. Our data suggest that it is the viscosity of the solvent which, reducing the conformational mobility, plays the most important role in determining the photoluminescence properties.

4. Experimental

4.1. Materials

All compounds were prepared by reacting 2,5-dibromothiophene-*S*,*S*-dioxide[8f] or 2,5-dibromo-3,4-dialkyl-thiophene-*S*,*S*-dioxide[8d,f] with the appropriate monostannane according to the modalities described in Ref. 2. Compounds **1**,**4** are described in Refs. 2,4, while compound **2** is described in Ref. 8d. The synthesis of compound **4** and of the corresponding intermediates, compounds **5**–**8**, is reported below.

4.1.1. 3-Cyclohexyl-thiophene (5). The title compound was prepared by the Grignard reaction between 3-bromothiophene and 2-cyclohexyl-magnesium bromide (from 2-cyclohexyl bromide, Aldrich) in the presence of nickel diphenylphosphinopropane, $Ni(dppp)Cl_2$ (Aldrich). Yield 65%; pale yellow oil; MS (70 eV, EI): *m*/*e* 166 (M^{+}). ^1H NMR ($CDCl_3$,TMS): δ (ppm)=7.23 (m, 1H); 6.98 (m, 1H); 6.91 (m, 1H), 2.6 (m, 1H); 2.0 (m, 2H); 1.75 (m, 3H); 1.3 (m, 5H). ^{13}C NMR ($CDCl_3$, TMS): δ (ppm)=149.1; 127.0; 124.9; 118.3; 39.6; 34.3; 26.6; 26.2. Anal. calcd for $C_{10}H_{14}S$: C, 72.23; H, 8.49. Found: C, 72.31; H, 8.52.

4.1.2. 2-Bromo-3-cyclohexyl-thiophene (6). The title compound was prepared by reacting compound **5** with

N-bromosuccinimide (Lancaster) in acetic acid–methylene chloride 1:1 (v:v). Yield 88%; pale yellow oil; MS (70 eV, EI): *m/e* 244, 246 ($M^{\cdot+}$). ^{1}H NMR ($CDCl_3$, TMS): δ (ppm)=7.18 (d, 1H, *J*=5.8 Hz); 6.82 (d, 1H, *J*=5.8 Hz); 2.7 (m, 1H); 1.80 (m, 5H); 1.3 (m, 5H). ^{13}C NMR ($CDCl_3$, TMS): δ (ppm)=146.7; 126.0; 125.3; 107.7; 39.0; 33.2; 26.6; 26.1. Anal. calcd for $C_{10}H_{13}BrS$: C, 48.99; H, 5.34. Found: C, 49.12; H, 5.36.

4.1.3. 3,3′-Di-cyclohexyl-2,2′-bithiophene (7). To 0.06 g (0.0025 mol) of magnesium turnings contained into a dry flask under N_2 stream was added first anhydrous diethyl ether (3 mL) and then **6** (1.0 g, 0.004 mol) in diethyl ether (1 mL) and the mixture was refluxed for 1 h. Then Ni(dppp)Cl_2 (0.33 g, 0.0006 mol) was added stepwise and the mixture refluxed for about 4 h. Afterwards the mixture was washed with water, the organic layer separated, dried over Na_2SO_4 and chromatographed on silica gel using cyclohexane as the eluant. 0.37 g (55% yield) of pure **7** were obtained. White solid, mp 96°C; MS (70 eV, EI): *m/e* 330 ($M^{\cdot+}$); λ_{max} (CH_2Cl_2)=267 nm. ^{1}H NMR ($CDCl_3$, TMS): δ (ppm)=7.31 (d, 2H, *J*=5.2 Hz); 7.04 (d, 2H, *J*=5.2 Hz); 2.6 (m, 2H); 1.80 (m, 10H); 1.3 (m, 10H). ^{13}C NMR ($CDCl_3$, TMS): δ (ppm)=147.5; 127.5; 126.1; 125.4; 38.1; 34.5; 26.7; 26.1. Anal. calcd for $C_{20}H_{26}S_2$: C, 80.48; H, 8.78. Found: C, 80.37; H, 8.81.

4.1.4. 5-Tributylstannyl-3,3′-di-cyclohexyl-2,2′-bithiophene (8). To a solution of **7** (0.4 g, 0.0012 mol) in anhydrous THF (3.5 mL) at *T*=−70°C was added dropwise BuLi (2.5 M in hexane, 0.48 mL, 0.0012 mol) and the mixture stirred for 1 h. Then the temperature was raised to room temperature and, after 2 h, 2-tributylstannyl chloride (0.406 g, 0.00125 mol) was added dropwise and the mixture stirred overnight. Then the crude product was chromatographed on Al_2O_3 using hexane as the eluant. 371 mg (50% yield) of a yellow oil was obtained. MS (70 eV, EI): *m/e* 619 ($M^{\cdot+}$); λ_{max} (CH_2Cl_2)=275 nm. ^{1}H NMR (CD_2Cl_2, TMS): δ (ppm)=7.27 (d, 1H, *J*=5.0 Hz); 7.01 (s, 1H), 6.99 (d, 1H, *J*=5.0 Hz); 1.8–1.1 (m, 38H); 0.9 (m, 9H). ^{13}C NMR ($CDCl_3$, TMS): δ (ppm)=148.3; 147.0; 136.9; 134.5; 133.2; 128.3; 126.2; 125.0; 38.1; 34.6; 34.5; 29.1; 27.3; 26.8; 26.7; 26.2; 26.1; 13.9; 11.0. Anal. calcd for $C_{32}H_{52}S_2Sn$: C, 62.03; H, 8.46. Found: C, 61.88; H, 8.48.

4.1.5. 3,3′,4‴,3⁗Tetracyclohexyl-3″,4″-di(*n*-hexyl)-2,2′:5′,2″:5″,2‴:5‴,2⁗-quinquethiophene-1″,1″-dioxide (4). The title compound was obtained from the cross coupling of **8** with 2,5-dibromo-3,4-dihexyl-thiophene-1,1-dioxide[8g] according to the method described in Ref. 8g. Yield: 90%. Orange solid, mp 185°C; MS (70 eV, EI): *m/e* 940 ($M^{\cdot+}$); λ_{max} (CH_2Cl_2)=455 nm. ^{1}H NMR ($CDCl_3$, TMS): δ (ppm)=7.69 (s, 2H), 7.35 (d, 2H, *J*=5.2 Hz); 7.04 (d, 2H, *J*=5.2 Hz); 2.65 (m, 6H); 1.9–1.1 (m, 56H); 0.9 (m, 6H). ^{13}C NMR ($CDCl_3$, TMS): δ (ppm)=148.6; 148.2; 136.4; 130.8; 129.9; 128.8; 127.8; 126.5; 126.3; 126.2; 38.3; 38.2; 34.6; 34.3; 31.5; 29.8; 28.5; 27.4; 26.6; 26.1; 26.0; 22.7; 14.2. Anal. calcd for $C_{56}H_{76}O_2S_5$: C, 82.70; H, 9.42. Found: C, 82.55; H, 9.39.

4.2. Computational methods

Ab Initio calculations were performed using the Gaussian98 series of programs.[12] The geometries were fully optimized by standard gradient techniques and the critical points checked by frequency analysis. Molecular Mechanics calculations were carried out using the MM3(96) program[13] parametrized as described in Section 1. UV transitions were calculated by ZINDO/S-C.I. (10x10) single point calculations on ab initio geometries using HyperChem integrated package.[14]

4.3. NMR measurement

The ^{1}H NMR spectra at variable temperatures were recorded with a Varian-Mercury spectrometer operating at 400 MHz. The samples were prepared under vacuum by condensing the appropriate quantity of CHF_2Cl and CF_2Cl_2 in an NMR tube immersed in liquid nitrogen and then sealing the tube with a flame. In the VT experiments the samples were dissolved in CD_2Cl_2 and cooled to the appropriate temperature by a flow of dry nitrogen precooled in the standard spectrometer heat exchanger immersed in liquid nitrogen. The temperatures were checked by substituting the sample before the measurements with a calibrated thermocouple in order to reduce the experimental error, that is estimated to be in the range of ±0.5°C. Line shape simulations of the ^{1}H traces were performed by using a PC version of the DNMR-6 programme[15] and the best fit was visually judged by superimposing the simulated and experimental traces.

4.4. Absorption and photoluminescence measurements

Absorption and photoluminescence spectra were recorded using a Perkin–Elmer Lambda 20 and a Perkin–Elmer LS 50 B spectrometer, respectively. The concentrations were in the range $2–5\times10^{-6}$ M in CH_2Cl_2 (absorbance 0.1–0.2). The excitation wavelengths were in the range 440–450 nm for all compounds.

Acknowledgements

The present work was partially supported by the project 'Nuovi emettitori di luce a semiconduttore organico' (CNR-5% Nanotecnologie).

References

1. *Handbook of Conductive Polymers*; Skotheim, T. A., Elsenbaumer, R. L., Reynolds, J. R., Eds.; Marcel Dekker: New York, 1998.
2. *Electronic Materials: The Oligomer Approach*; Müllen, K., Wegner, G., Eds.; Wiley-VCH: New York, 1998.
3. *Handbook of Oligo and Polythiophenes*; Fichou, D., Ed.; Wiley-VCH: New York, 1999.
4. Bao, Z.; Rogers, J. A.; Katz, H. E. *J. Mater. Chem.* **1999**, *9*, 1895–1904.
5. Garnier, F. *Acc. Chem. Res.* **1999**, *32*, 209–215.
6. Mitschke, U.; Bäuerle, P. *J. Mater.Chem.* **2000**, *10*, 1471–1507.
7. (a) Charas, A.; Morgado, J.; Marthinho, J. M. G.; Alcácer, L.; Cacialli, F. *Chem. Commun.* **2001**, 1216–1217. (b) Barbarella,

G.; Favaretto, L.; Zambianchi, M.; Pudova, O.; Arbizzani, C.; Bongini, A.; Mastragostino, M. *Adv. Mater.* **1998**, *10*, 551–554.

8. (a) Barbarella, G.; Favaretto, L.; Sotgiu, G.; Zambianchi, M.; Bongini, A.; Arbizzani, C.; Mastragostino, M.; Anni, M.; Gigli, G.; Cingolani, R. *J. Am. Chem. Soc.* **2000**, *122*, 11971–11978. (b) Gigli, G.; Inganä, O.; Anni, M.; De Vittorio, M.; Cingolani, R.; Barbarella, G.; Favaretto, L. *Appl. Phys. Lett.* **2001**, *78*, 1493–1495. (c) Gigli, G.; Barbarella, G.; Favaretto, L.; Cacialli, F.; Cingolani, R. *Appl. Phys. Lett.* **1999**, *75*, 439–441. (d) Barbarella, G.; Favaretto, L.; Sotgiu, G.; Zambianchi, M.; Fattori, V.; Cocchi, M.; Cacialli, F.; Gigli, G.; Cingolani, R. *Adv. Mater.* **1999**, *11*, 1375–1379. (e) Barbarella, G.; Favaretto, L.; Sotgiu, G.; Antolini, L.; Gigli, G.; Cingolani, R.; Bongini, A. *Chem. Mater.* **2001**, *13*, 4112–4122. (f) Barbarella, G.; Favaretto, L.; Sotgiu, G.; Zambianchi, M.; Antolini, L.; Pudova, O.; Bongini, A. *J. Org. Chem.* **1998**, *63*, 5497–5506. (g) Barbarella, G.; Favaretto, L.; Sotgiu, G.; Zambianchi, M.; Arbizzani, C.; Bongini, A.; Mastragostino, M. *Chem. Mater.* **1999**, *11*, 2533–2541.
9. (a) Bongini, A.; Bottoni, A. *J. Phys. Chem. A* **1999**, *103*, 6800–6804, and references therein. (b) Diaz-Quijada, G. A.; Weinberg, N.; Holdcroft, S.; Pinto, B. M. *J. Phys. Chem. A* **2002**, *106*, 1266–1276, and references therein. (c) Diaz-Quijada, G. A.; Weinberg, N.; Holdcroft, S.; Pinto, B. M. *J. Phys. Chem. A* **2002**, *106*, 1277–1285, and references therein.
10. Della Sala, F.; Heinze, H. H.; Görling, A. *Chem. Phys. Lett.* **2001**, *339*, 343–350.
11. Lanzani, G.; Cerullo, G.; De Silvestri, S.; Barbarella, G.; Sotgiu, G. *J. Chem. Phys.* **2001**, *115*, 1623–1625.
12. Frisch, M. J.; Trucks, G. W.; Schlegel, H. B.; Scuseria, G. E.; Robb, M. A.; Cheeseman, J. R.; Zakrzewski, V. G.; Montgomery, J. A. Jr; Stratmann, R. E.; Burant, J. C.; Dapprich, S.; Millam, J. M.; Daniels, A. D.; Kudin, K. N.; Strain, M. C.; Farkas, O.; Tomasi, J.; Barone, V.; Cossi, M.; Cammi, R.; Mennucci, B.; Pomelli, C.; Adamo, C.; Clifford, S.; Ochterski, J.; Petersson, G. A.; Ayala, P. Y.; Cui, Q.; Morokuma, K.; Malick, D. K.; Rabuck, A. D.; Raghavachari, K.; Foresman, J. B.; Cioslowski, J.; Ortiz, J. V.; Baboul, A. G.; Stefanov, B. B.; Liu, G.; Liashenko, A.; Piskorz, P.; Komaromi, I.; Gomperts, R.; Martin, R. L.; Fox, D. J.; Keith, T.; Al-Laham, M. A.; Peng, C. Y.; Nanayakkara, A.; Gonzalez, C.; Challacombe, M.; Gill, P. M. W.; Johnson, B.; Chen, W.; Wong, M. W.; Andres, J. L.; Gonzalez, C.; Head-Gordon, M.; Replogle, E. S.; Pople, J. A. *Gaussian98, Revision A.7*; Gaussian, Inc.: Pittsburgh, PA, 1998.
13. Allinger, N. L. *QCPE*; Indiana University: Bloomington, IN 47405, USA.
14. *HyperChem rel 7.0* from HyperCube: Waterloo, Ont., Canada.
15. *QCPE program n. 633*; Indiana University: Bloomington, USA.